

# Influence of the measurement configuration on the results of Raman microspectroscopy of human hair

N.N. Brandt, E.I. Travkina, E.V. Mikhal'chik, A.Yu. Chikishev

**Abstract.** Increasing interest in spectroscopic studies of human hair raises the question about the accuracy of measurement of their spectra and requires optimisation of experimental facilities. An original method of obtaining transverse hair sections without using a microtome and chemical influence is proposed. The results obtained by confocal Raman microspectroscopy of human hair differently oriented with respect to the optical axis of the measuring setup are compared. It is shown that, in addition to expected changes in the spectra measured at different distances from the hair periphery in the direction to its centre, the spectra measured in the case of hair excitation perpendicular and parallel to its axis are also considerably different.

**Keywords:** Raman microspectroscopy, Raman mapping of human hairs, hair cross section preparation.

## 1. Introduction

Hair is a skin appendage, 80%–90% of which consist of proteins (keratins). The main part of hair forms a cortical substance (cortex), which determines the mechanical properties of hair due to the structural organisation of water-insoluble macromolecular keratins into fibrils. Fibrils are embedded in a matrix containing low-molecular keratins. The hair surface is covered with a cuticle consisting of several layers. The cuticle fulfils several functions; in particular, it provides mechanical protection and controls the content of water in the hair fibre (see, for example, [1]). Low-molecular soluble keratins comprise only a small part compared to fibrous keratins. They are contained mainly in the hair cortex and form the matrix, which supports the hair structure due to the bonds between proteins [2–4]. Low-molecular keratins include more than 20 protein families differing in molecular mass (5–60 kDa) and in content of glycine, tyrosine, and cysteine [5].

Despite the fact that human hair is accessible for investigation and has been studied by various modern methods [6, 7], many questions related to the hair structure remain topical. In particular, a highly resistive layer (a resistive base attached to the cuticle) preventing penetration of environmental molecules into the cortex was recently found in [8].

Interest in the study of human hair is also related to the fact that hair, which is not exactly a living tissue, responds to external impacts [9, 10] by structural changes similar to changes in skin keratins [11]. Therefore, hair can be used to search markers of keratin destruction under action of, for example, UV radiation [12].

One of the most important modern methods of scientific research of hair is Raman scattering spectroscopy. In recent years, industrial confocal Raman microspectrometers, which allow Raman mapping of samples with a 3D spatial resolution of up to 1  $\mu\text{m}$ , have found wide use in scientific investigations. Since the human hair cuticle thickness is of the order of several micrometres, the use of Raman microspectrometry for studying these objects is fully justified. This method came into use for studying the hair structure at the beginning of this century (see, for example, [13]). Subsequent works refined the obtained results and revealed new structural features of hairs of different types [14–16]. At present, Raman spectroscopy is, as before, widely used to analyse the human hair structure [17, 18]. However, some methodological questions related to the measurement of Raman spectra of hairs still remain open. In some works, a hair is cut by a microtome after fixation in, for example, epoxy resin [13, 15], and the spectra are measured at the hair cross section with a lateral (transverse) resolution. In other works, a hair is positioned horizontally and fixed on a substrate (see, e.g., [19]). Laser radiation is coupled in vertically, i.e., perpendicular to the hair axis, and the confocal light collection geometry makes it possible to achieve an axial (longitudinal) resolution. In [14], a horizontally positioned hair was first covered with a cover glass, and then an oil immersion objective was moved down to it. Unfortunately, the reasons for choosing one or another experimental geometry in the mentioned papers are not reported, which sometimes makes it difficult to comparatively analyse the experimental results.

Therefore, in the present work we compare the spectral data obtained by confocal Raman microspectroscopy using different experimental configurations.

## 2. Materials and methods

### 2.1. Raman microspectroscopy method

Raman spectra were measured using a confocal DXR Raman Microscope (Thermo Scientific). Excitation was performed by a cw single-mode frequency-stabilised diode laser emitting at a wavelength of 780 nm. The radiation power on the sample was 24 mW. The radiation was focused on the sample by an Olympus LMPlanFL N 50X/0.5 BD objective with a working distance of 10.6 mm. The focused beam spot was

N.N. Brandt, E.I. Travkina, A.Yu. Chikishev Faculty of Physics, Lomonosov Moscow State University, Leninskie Gory, 119991 Moscow, Russia; e-mail: brandt@physics.msu.ru;

E.V. Mikhal'chik Federal Research and Clinical Center of Physical-Chemical Medicine, ul. Malaya Pirogovskaya 1a, 119435 Moscow, Russia

Received 2 October 2021

*Kvantovaya Elektronika* 52 (1) 36–41 (2022)

Translated by M.N. Basieva

1.6  $\mu\text{m}$  in diameter. The single spectrum accumulation time was 15 min. The measurements were performed in the spectral range 50–3500  $\text{cm}^{-1}$  with a spectral resolution of 4  $\text{cm}^{-1}$ . The lateral and axial resolutions of the microscope were 2 and 6  $\mu\text{m}$ , respectively. The sample images were recorded using a colour digital video camera with a 1024  $\times$  768 pixel matrix.

Raman spectra always contain a background signal, which changes even in the case of consecutive measurements of two spectra at one point of the sample. Because of this, to compare spectra in detail, we used the background correction procedure described in [20]. This procedure includes minimisation of the root-mean-square deviation of one of the compared spectra from the other in the spectral ranges free of conformation-sensitive protein lines (250–450, 570–620, 750–820, 960–1020, 1060–1200, 1350–1580, and 1750–2000  $\text{cm}^{-1}$ ) and ensures an almost complete equality of background signals in the compared spectra.

## 2.2. Preparation of samples

In the experiments we used a grey hair of a healthy 60-year-old donor. The measurements were performed in the following two configurations.

*Vertical hair position.* Obtaining a transverse hair section is an independent task. This is usually done using a microtome. However, in this case one has to immerse a hair (a hair lock) into a stabilising medium, for example, into epoxy resin, which should be in the solid state at the instant of cutting. We used an original method of transverse cutting of a hair without using a microtome and foreign substances, which could penetrate into the hair structure and affect its composition.

The end part of a hair  $\sim 1$  cm long was placed in a Petri dish with liquid nitrogen for several seconds. The hair in the frozen region was broken, and its edge in some cases was approximately plane. We selected samples with a cylindrical shape, a length of  $\sim 5$  mm, and almost plane edges perpendicular to the hair axis. These samples were attached by their side surfaces to a scotch type parallel to each other so that the plane edge of each sample overhung the scotch tape edge by  $\sim 1$  mm. Then, the scotch tape was glued to the vertical surface of a thick plane-parallel glass plate, which was mounted on the objective table of a Raman microscope, and the sample edges turned out to be perpendicular to the optical axis of the objective. With lateral movement of the sample, its surface remained in the focal plane of the objective.

*Horizontal position of the hair.* A hair about 1 cm long was placed horizontally on a substrate over an aperture 2 mm in diameter. The edges of the sample were glued to the substrate, and the system was mounted on an objective table of a Raman microscope. This configuration ensures rigid fixation of the sample and the absence of background signals from the substrate in the spectrum.

## 3. Results and discussion

Figure 1a shows two typical spectra measured upon focusing of exciting radiation on the surface of a horizontally placed hair. In addition to the background signal correction described in the previous section, the spectra are vertically shifted with respect to each other for convenience of comparison. The used parameters of the objective and confocal aperture of the microscope provide an axial resolution of 6  $\mu\text{m}$ . Thus, the scattered radiation is collected from the region adjacent to the hair surface, which has a depth of up to 3  $\mu\text{m}$ ,

a diameter of 2  $\mu\text{m}$ , and a hemispheroidal shape. The hair was not preliminarily treated, and the distance along its surface between points 1 and 2, at which the spectra were measured, was several millimetres. Figure 1b presents the difference between spectra 1 and 2 (without allowance for the vertical shift). One can clearly see that the spectra almost completely coincide. The deviation of the difference curve from zero illustrates the difference ( $\sim 1\%$ ) between the spectra measured at different surface points of one and the same sample.

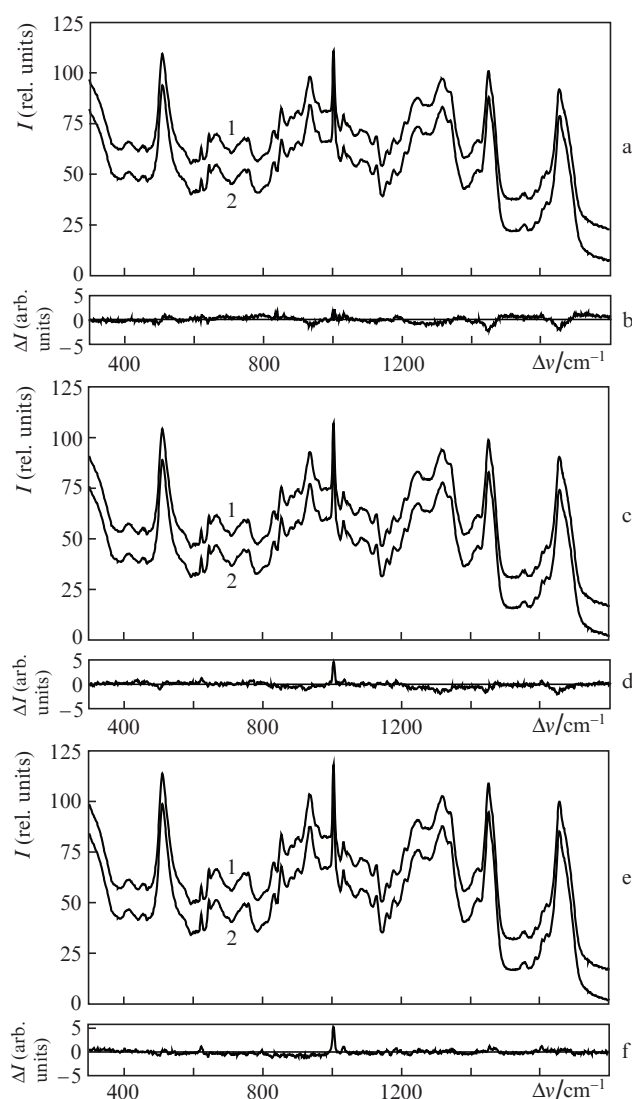


**Figure 1.** (a) Raman spectra 1 and 2 measured at two different points of a horizontally positioned hair in the case of excitation focusing on its surface and (b) difference between these spectra; (c) Raman spectra measured in the same geometry (1) after and (2) before hair treatment in liquid nitrogen and (d) difference between these spectra; (e) Raman spectra measured in the case of excitation focusing at a depth of 10  $\mu\text{m}$  from the surface of a horizontally positioned hair (1) after and (2) before treatment in liquid nitrogen and (f) difference between these spectra.

The curves in Figs 1c and 1d, as well as in Figs 1e and 1f, are similar to the curves shown in Figs 1a and 1b. The spectra are processed by the same technique. Figure 1c shows the spectra measured in the case of focusing of exciting radiation on the surface of a hair positioned horizontally as well. Spectrum 1 corresponds to an untreated hair (spectrum 2 in

Fig. 1a), while spectrum 2 is measured for a hair kept in liquid nitrogen for 30 s and then returned to room temperature. Comparison of the difference curves given in Figs 1b and 1d shows that the influence of liquid nitrogen on the hair protein structures is minimal. Attention is drawn to only a slight change in the intensity of the phenylalanine line at a frequency of  $1003\text{ cm}^{-1}$ . This line is usually considered as conformationally insensitive and is used as a reference for normalisation of Raman spectra. Similar minimal differences are observed between the spectra of the same samples measured at a depth of  $10\text{ }\mu\text{m}$  from the hair surface (Fig. 1e). In this case, the Raman signal is collected from the region inside a spheroid with a height of  $6\text{ }\mu\text{m}$ , a diameter of  $2\text{ }\mu\text{m}$ , and a centre at the mentioned depth.

The presented data on the volume from which the Raman signal is collected allow us to conclude that, even when the exciting radiation is focused on the hair surface, a considerable part of the signal is emitted from the cortex rather than from the cuticle because the characteristic thickness of the cuticle is  $\sim 1\text{ }\mu\text{m}$  [7]. Because of this, the spectra measured at the hair surface (spectrum 1 in Fig. 1c and at a depth of  $10\text{ }\mu\text{m}$  (spectrum 1 in Fig. 1e) almost coincide.

It is necessary to note that, in most light collection configurations, the axial resolution of Raman microspectroscopy is lower than the lateral resolution. The lateral resolution for the spectra shown in Fig. 1 ( $2\text{ }\mu\text{m}$ ) is threefold better than the axial resolution ( $6\text{ }\mu\text{m}$ ). The choice of a high-magnification ( $100\times$ ) objective and a decrease of the confocal aperture diameter make it possible to improve the axial resolution to  $2\text{ }\mu\text{m}$ , but the working distance of the objective and the signal-to-noise ratio in this case are considerably smaller, which does not allow one to obtain high-quality spectra.

An additional drawback of the horizontal hair position is that it is impossible to precisely determine correction factors to compare the spectra measured in the confocal regime at different depths from the hair surface. The horizontally positioned hair is a cylindrical lens, which considerably changes the laser beam focusing geometry. Since the diameters and refractive indices of hair samples are different, the corrections to the spectra should be individually calculated for each sample. In addition, the spectral corrections will considerably depend on the hair absorption coefficients at different wavelengths, the measurement of which is a separate problem (see, e.g., [21]).

Figure 2a shows a series of spectra measured upon focusing of exciting radiation on a hair edge formed by cleaving in liquid nitrogen. The spectra are processed similar to the spectra shown in Fig. 1 and are vertically shifted for convenience of comparison. Spectrum 1 is obtained in the case of radiation focusing on the hair edge along the hair axis so that the Raman signal is collected from the volume of a hemispheroid that lies inside the hair and borders its side surface. The plane surface of the hemispheroid  $2\text{ }\mu\text{m}$  in diameter coincides with the hair edge surface. The hemispheroid height is  $\sim 3\text{ }\mu\text{m}$ . Note that the laser beam waist in this geometry coincides with the hair edge surface independently of its lateral position. In the approximation that the hair absorption coefficient at the excitation wavelength only slightly depends on the radial coordinate, the Raman spectra measured at different points can be compared with each other without additional corrections. Moreover, the use of long-focal length objectives in the considered geometry is unreasonable. However, for correct

comparison of the spectra considered in the present work, we in all experiments used the same long-focal length objective as in the case of Raman microspectroscopy of a hair in the horizontal position (Fig. 1). The spatial resolution in the case of a vertically positioned hair is determined by the lateral rather than axial resolution and may reach fractions of a micrometre. The spatial resolution for the configuration used for measuring the spectra shown in Fig. 2a was  $2\text{ }\mu\text{m}$ , which slightly exceeds the hair cuticle thickness. Spectra 2–5 are measured at focal points shifted from the periphery to the hair centre by 2, 4, 6, and  $8\text{ }\mu\text{m}$ , respectively, with respect to the point used for spectrum 1.

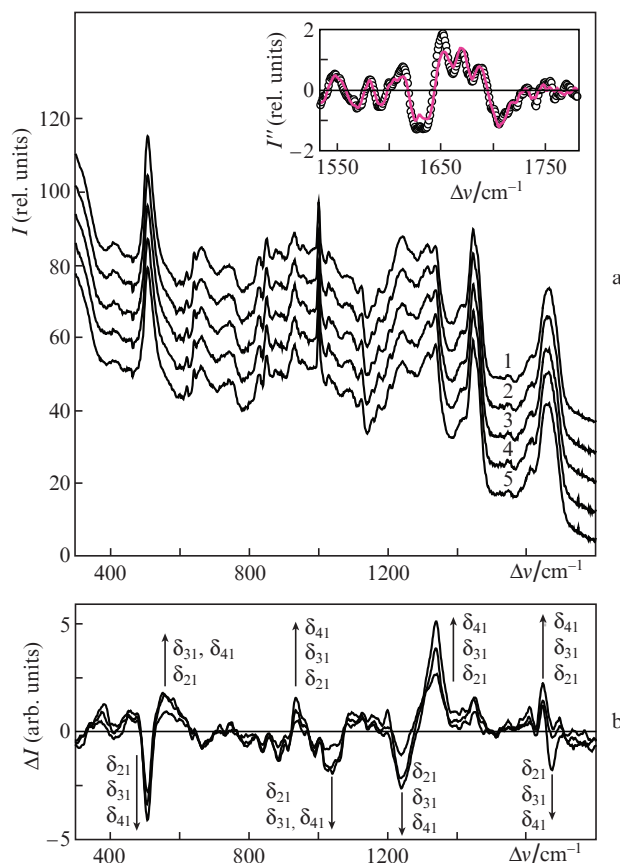


**Figure 2.** (Colour online) (a) Raman spectra of a vertically positioned hair in the case of excitation focusing on the hair cross section at points 1, 2, 3, 4, and 5 (see Fig. 3 below) spaced from each other by  $2\text{ }\mu\text{m}$  and (b) differences between spectra ( $\delta_{21}$ ) 2 and 1, ( $\delta_{31}$ ) 3 and 1, and ( $\delta_{41}$ ) 4 and 1. The inset in Fig. 2a shows the second derivatives  $I''$  of spectra (solid line) 1 and (circles) 5.

Figure 3 shows the microphotograph of the considered hair cross section, which was made by a long-focal length objective used for laser excitation of the Raman spectra. Circles 1–5 are the projections of hemispheroids from which the Raman signals were collected onto the image plane. The numeration of the circles corresponds to the numeration of the spectra. One can see that spectrum 1 should belong to the cuticle, spectrum 2 corresponds to the linear combination of the cuticle and cortex spectra, and spectra 3–5 are the cortex spectra.

For convenient analysis of the spectra, Fig. 2b presents the differences between spectra 2, 3, and 4 and spectrum 1,

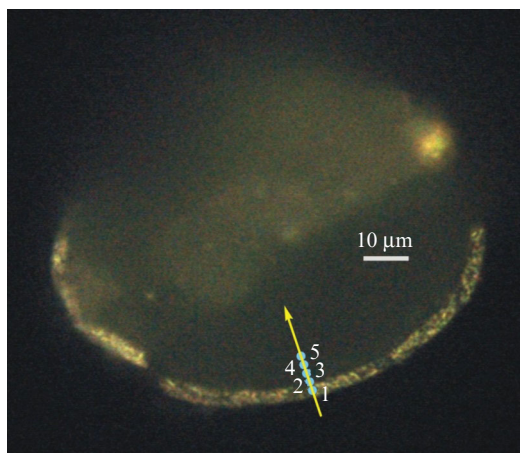


**Figure 3.** (Colour online) Microphotograph of a hair cross section made using an Olympus LMPlanFL N 50X/0.5 BD long-focal length objective. Figures denote the focal points of the excitation laser beam used for measuring the spectra with the corresponding numbers shown in Fig. 2.

which are denoted as  $\delta_{21}$ ,  $\delta_{31}$ , and  $\delta_{41}$ , respectively. All spectral differences are smoothed using the Savitzky–Golay filter. The difference between the fifth and first spectra almost coincides with difference  $\delta_{41}$  and is not shown in Fig. 2b. Pronounced differences between the spectra are observed at frequencies of 508, 550, 935, 1040, 1243, 1338, 1649, and 1676  $\text{cm}^{-1}$  (these differences are indicated by arrows in Fig. 2b). The lines at frequencies of 508 and 550  $\text{cm}^{-1}$  belong to the stretching vibrations of disulphide bridges in the gauche-gauche-gauche (ggg) and trans-gauche-trans (tgt) conformations, respectively (see, for example, [22]). Some authors believe that the band at a frequency of 935  $\text{cm}^{-1}$  is caused by the skeletal vibrations of the polypeptide chain (N–C $_{\alpha}$ –C bending vibrations) and characterises the content of helix structures. This frequency can also correspond to the C–N and N–C $_{\alpha}$  stretching vibrations and the CH $_3$  rocking vibrations [23]. The line at 1040  $\text{cm}^{-1}$  belongs to the S=O symmetric stretching vibrations of cysteic acid. An increase in the intensity of this line can be related to a decrease in the concentration of free thiols [24]. The intensity of the amide III line at a frequency of 1243  $\text{cm}^{-1}$  characterises the disordered structure in protein molecules (see, e.g., [19]). One can see from Fig. 2a that the pronounced changes near 1340  $\text{cm}^{-1}$  (Fig. 2b) are related to the changes in the intensities of two peaks at frequencies of 1316 and 1338  $\text{cm}^{-1}$ . The first line belongs to the C $_{\alpha}$ –H vibrations, and the second line corresponds to the CH $_2$  bending vibrations and tryptophan vibrations [25].

To identify the spectral components of the amide I line near 1660  $\text{cm}^{-1}$ , the inset in Fig. 2a presents the second derivatives of the first and the last spectra in the series (the derivatives of spectra 2–4 have the same spectral features in this region). The second derivatives of the spectra clearly exhibit three main components of the amide I line at frequencies of 1652, 1670, and 1688  $\text{cm}^{-1}$ . The relative intensities of these components are proportional to the content of  $\alpha$ -helixes,  $\beta$ -sheets, and  $\beta$ -turns, respectively [26]. The line at 1688  $\text{cm}^{-1}$  can also be related to the vibrations of the amide groups of the asparagine and glutamine side chains [24]. Note that the spectral differences at frequencies of 935 (N–C $_{\alpha}$ –C), 1316

(C $_{\alpha}$ –H), and 1652 ( $\alpha$ -helix)  $\text{cm}^{-1}$  well correlate with each other.

Thus, when passing from cuticle to cortex, we note the following most important changes.

- The concentration of disulphide bonds decreases and a part of disulphide bridges transforms from ggg to tgt configuration.

- The amount of  $\alpha$ -helices in molecules increases due to a decrease in the content of  $\beta$ -structured and disordered elements.

- The concentration of free thiols increases.

All the listed conclusions completely agree with available literature data (see, e.g., [27]).

For comparison, Fig. 4a shows the hair spectra measured in the horizontal (spectrum 1 in Fig. 1a) and vertical (spectrum 1 in Fig. 2a) configurations, and Fig. 4b presents the difference between the first and second spectra. One can see that the main differences between the spectra consist in the different intensities of lines near frequencies of 508, 897, 935, 1001, 1243, 1316, 1652, and 1688  $\text{cm}^{-1}$ . First of all, the distinctions between the spectra measured in the horizontal and vertical positions of hairs can be related to the polarisation sensitivity of the Raman signal. In the case of measurements with the Raman microscope used in the present work, the exciting radiation is depolarised. Therefore, the exciting radiation for the vertically positioned hair is polarised perpendicular to the hair axis, while in the case of the horizontal hair position half of exciting photons is on average polarised parallel to the hair axis ( $x$  axis) and the other half is polarised perpendicular to it ( $y$  axis). The scattered signal contains both the  $x$  and  $y$  field components. The Raman spectra of a human hair in [28] were measured upon excitation by  $x$ - and  $y$ -polarised light at a wavelength of 785 nm. For each polarisation, the analyser in the recording channel was also oriented either parallel (along the  $x$  axis) or perpendicular (along the  $y$  axis) to the hair axis. As a result, the  $S_{xx}$ ,  $S_{xy}$ ,  $S_{yx}$ , and  $S_{yy}$  spectra were measured (the first and second subscripts correspond to the orientation of the polariser and the analyser, respectively). In the absence of an analyser upon depolarised excitation, the spectrum recorded for the horizontally positioned hair can be estimated as the sum  $S_h = 0.5(S_{xx} + S_{xy} + S_{yx} + S_{yy})$ . The spectrum measured for the vertically positioned hair is estimated as  $S_v = S_{yx} + S_{yy}$ . We used the results of work [28] and calculated the spectral difference  $S_h - S_v$  (Fig. 4c). One can see that all spectral features of this difference (the doublet at frequencies of 897 and 935  $\text{cm}^{-1}$  and the lines at 1316 and 1652  $\text{cm}^{-1}$ ) exist in the spectral difference shown in Fig. 4b and characterise the polarisation sensitivity of  $\alpha$ -helices in the composition of protein molecules, whose axes are directed mainly along the hair axis. Note that the polarisation sensitivity of amide lines also manifests itself in the IR spectra of individual collagen fibrils [29].

The other spectral differences shown in Fig. 4b can be caused by the following. As was noted above, the contribution to the Raman signal in the case of the horizontal hair position is made by both the cuticle and the cortex (dashed curve in Fig. 4a), while in the case of the vertically positioned hair this contribution is made only by the cuticle (solid curve). Therefore, the spectral difference should characterise the change in the content of the structural elements of the molecule with moving from the hair surface to its centre. Similar changes should exist in the spectral difference  $\delta_{41}$  in Fig. 4d (difference between the spectra measured in the

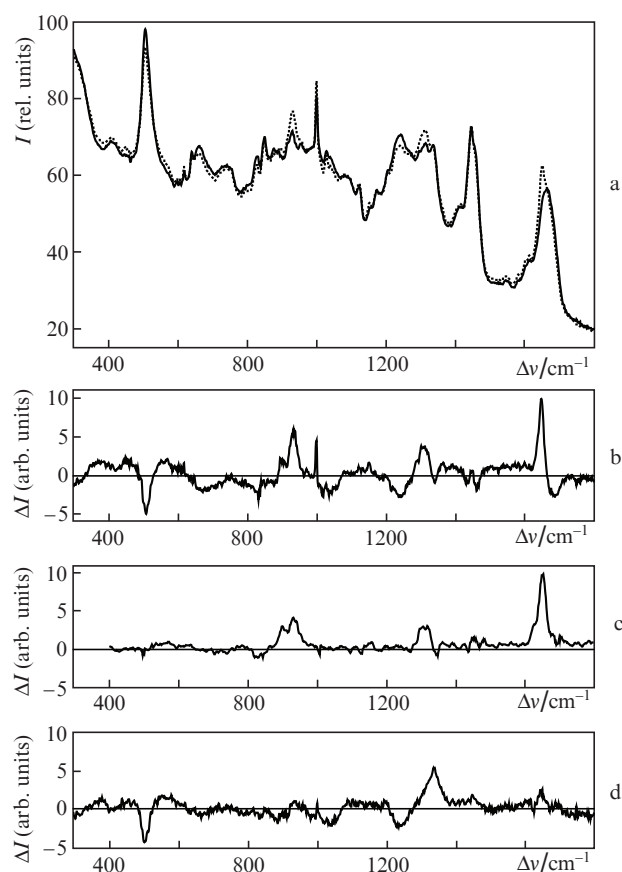


**Figure 4.** (a) Raman spectra measured in the case of excitation focusing on (dashed curve) the surface of a horizontally positioned hair and (solid curve) point 1 of a vertically positioned hair (Fig. 3), as well as (b) difference between these spectra; (c) difference  $S_h - S_v$  calculated using the results of work [28] (see the text), and (d) difference between the Raman spectra measured at points 4 and 1 shown in Fig. 3.

vertical configuration at points 4 and 1 shown in Fig. 3). Indeed, both spectral differences (in Figs 4b and 4d) exhibit an increase in the concentration of amino acid residues of phenylalanine ( $1001\text{ cm}^{-1}$ ) and a decrease in the content of disulphide bonds ( $508\text{ cm}^{-1}$ ) and disordered structural elements ( $1243\text{ cm}^{-1}$ ), which corresponds to the literature data [24].

#### 4. Conclusions

In this work, we proposed a method of preparation of hair cross section specimens without using fixing agents, namely, by freezing in liquid nitrogen. It is shown that the freezing procedure does not affect the spectral characteristics of hairs and, hence does not change the hair structure. The Raman spectra for studying the dependences of the parameters of the hair molecular structure on the radial coordinate can be measured with a spatial resolution exceeding the resolution of confocal measurements in the case of the horizontal hair position. Comparison of the spectra measured with radiation focusing on the surface of a horizontally positioned hair and on the cuticle in the hair cross section allowed us to identify the polarisation-sensitive lines in the hair spectra and to determine the change in the content of structural protein elements in the cuticle with respect to the cortex. The cross section of a vertically positioned hair can be studied

using commercially available confocal systems with a sub-micron resolution determined by the size of the excitation laser beam waist, which is considerably smaller than the cuticle thickness. In this case, the spectra are free of distortions caused by the hair surface curvature and by changes in scattering and absorption of radiation with focusing into the hair depth, which must be taken into account in the case of confocal probing of a horizontally positioned hair. On the other hand, the choice of the horizontal configuration is necessary to perform polarisation-sensitive measurements, which make it possible to determine the dominant orientation of  $\alpha$ -helix structures in hair proteins with respect to the hair axis.

**Acknowledgements.** This work was performed using equipment purchased at the expense of the Moscow State University Development Programme and was partially supported by the Russian Foundation for Basic Research (Grant No. 20-02-00932).

#### References

- Gadzhigoroeva A.G. *Klinicheskaya trikhologiya* (Clinical Trichology) (Moscow: Prakticheskaya Meditsina, 2014).
- Leszek J.W. *J. Am. Acad. Dermatol.*, **48** (6), 106 (2003). DOI: 10.1067/mjd.2003.276.
- Araujo R., Fernandes M., Cavaco-Paulo A., Gomes A. *Adv. Biochem. Eng. Biotechnol.*, **125**, 121 (2011). DOI: 10.1007/10\_2010\_88.
- Miranda-Vilela A.L., Botelho A.J., Muehlmann L.A. *Int. J. Cosmet. Sci.*, **36** (1), 2 (2014). DOI: 10.1111/ics.12093.
- Rogers M.A., Langbein L., Winter H., Beckmann I., Praetzel S., Schweizer J. *J. Invest. Dermatol.*, **122** (1), 147 (2004). DOI: 10.1046/j.0022-202X.2003.22128.x.
- Rogers G.E. *Cosmetics*, **6** (2), 32 (2019). DOI: 10.3390/cosmetics6020032.
- Fellows A.P., Casford M., Davies P. *Appl. Spectrosc.*, **74** (12), 1540 (2020). DOI: 10.1177/0003702820933942.
- Takahashi T. *Int. J. Cosmet. Sci.*, **43** (2), 254 (2021). DOI: 10.1111/ics.12691.
- Osorio F., Tosti A.J. *J. Cosmet. Dermatol.*, **24** (11), 533 (2011).
- Franca-Stefoni S.A., Dario M.F., Sa-Dias T.C., Bedin V., de Almeida J.A., Baby A.R., Velasco M.V.R. *J. Cosmet. Dermatol.*, **14** (3), 204 (2015). DOI: 10.1111/jocd.12151.
- Chavanas S., Bodemer C., Rochat A., Hamel-Teillac D., Ali M., Irvine A.D., Bonafé J.-L., Wilkinson J., Täieb A., Barrandon Y., Harper J.I., de Prost Y., Hovnanian A. *Nat. Genet.*, **25**, 141 (2000). DOI: 10.1038/75977.
- Pande C.M., Jachowicz J.J. *J. Soc. Cosmet. Chem.*, **44**, 109 (1993).
- Kuzuhara A. *Biopolymers*, **79** (4), 173 (2005). DOI: 10.1002/bip.20329.
- Zhang G., Senak L., Moore D.J. *J. Biomed. Opt.*, **16** (5), 056009 (2011). DOI: 10.1117/1.3580286.
- Kuzuhara A. *J. Mol. Struct.*, **1047**, 186 (2013). DOI: 10.1016/j.molstruc.2013.04.079.
- Pudney P.D.A., Bonnist E.Y.M., Mutch K., Stanfield S. *Appl. Spectrosc.*, **67** (12), 1408 (2013). DOI: 10.1366/13-07086.
- Dos Santos J.D., Edwards H.G.M., Oliveira L.F.C. *Heliyon*, **5** (5), e01582 (2019). DOI: 10.1016/j.heliyon.2019.e01582.
- Lam S.E., Mat Nawi S.N., Sani A., Khandaker M.U., Bradley D.A. *Sci. Rep.*, **11**, 1 (2021). DOI: 10.1038/s41598-021-86942-4.
- Schlücker S., Liang C., Strehle K.R., DiGiovanna J.J., Kraemer K.H., Levin I.W. *Biopolymers*, **82** (6), 615 (2006). DOI: 10.1002/bip.20515.
- Brandt N.N., Chikishev A.Yu., Chulichkov A.I., Ignatiev P.A., Lebedenko S.I., Voronina O.V. *Laser Phys.*, **14** (11), 1386 (2004).
- Bashkatov A.N., Genina E.A., Kochubei V.I., Tuchin V.V. *Quantum Electron.*, **36** (12), 1111 (2006) [*Kvantovaya Elektron.*, **36** (12), 1111 (2006)].
- Sugeta H., Go A., Miyazawa T. *Bull. Chem. Soc. Japan*, **46** (11), 3407 (1973). DOI: 10.1246/bcsj.46.3407.

23. Tuma R. *J. Raman Spectrosc.*, **36** (4), 307 (2005).  
DOI:10.1002/jrs.1323.
24. Church J.S., Corino G.L., Woodhead A.L. *Biopolymers*, **42** (1), 7 (1997); [https://doi.org/10.1002/\(SICI\)1097-0282\(199707\)42:1<7::AID-BIP2>3.0.CO;2-S](https://doi.org/10.1002/(SICI)1097-0282(199707)42:1<7::AID-BIP2>3.0.CO;2-S).
25. Carter E.A., Fredericks P.M., Church J.S., Denning R.J. *Spectrochim. Acta*, **50** (11), 1927 (1994).  
DOI: 10.1016/0584-8539(94)80205-x.
26. Lefevre T., Rousseau M.-E., Pezolet M. *Biophys. J.*, **92** (8), 2885 (2007). DOI: 10.1529/biophysj.106.100339.
27. Fedorkova M.V., Brandt N.N., Chikishev A.Yu., Smolina N.V., Balabushevich N.G., Gusev S.A., Lipatova V.A., Botchey V.M., Dobretsov G.E., Mikhailchik E.V. *J. Photochem. Photobiol. B: Biology*, **164**, 43 (2016). DOI: 10.1016/j.jphotobiol.2016.09.021.
28. Ackermann K.R., Koster J., Schlücker S. *J. Biophotonics*, **1** (5), 419 (2008). DOI: 10.1002/jbio.200810015.
29. Bakir G., Girouard B.E., Wiens R., Mastel S., Dillon E., Kansiz M., Gough K.M. *Molecules*, **25** (18), 4295 (2020).  
DOI: 10.3390/molecules25184295.